ACADEMIA ROMÂNĂ
Revue Roumaine de Chimie
http://web.icf.ro/rrch/

Rev. Roum. Chim.,
2022, *67*(3), 197–205
DOI: 10.33224/rrch.2022.67.3.08

PHYSICOCHEMICAL PROPERTIES AND ADSORPTION PERFORMANCES OF TEXTILE WASTE BASED HYDROLYZED CELLULOSE-PVDF COMPOSITES

Huseyin GUMUS[a,*] and Bulent BUYUKKIDAN[b]

[a] Osmaneli Vocational School, Bilecik Seyh Edebali University 11500, Osmaneli, Bilecik/Turkey
[b] Department of Chemistry, Kutahya Dumlupinar University, Kutahya/Turkey

Received January 15, 2022

The concepts of industrial waste materials, environmental pollution, and raw material requirement are related to each other, and one is both the result and solution of the other. In this study, sulfuric acid hydrolyzed cellulose separated from textile waste products was used to obtain composites with poly(vinylidene fluoride). The interaction of polymer and cellulose was confirmed by FT-IR and XRD analysis. The surface area and properties of composites were analyzed by SEM imaging and BET techniques respectively. The dye removal performance of hydrolyzed cellulose contained poly(vinylidene fluoride) composite was investigated from an aqueous solution. Both analysis and adsorption results showed that 50% hydrolyzed cellulose and 50% poly(vinylidene fluoride) mixed well and resulted in convenient composite material with a 15.83 m^2/g surface area. While 75% hydrolyzed cellulose containing sample showed low physical strength, 76.37 $mg.g^{-1}$ dye removal capacity was recorded at pH 7.5 for 50% hydrolyzed cellulose - poly(vinylidene fluoride) composite. New kinds of composite material have been developed and tested for water remediation by reusing textile wastes with recycling.

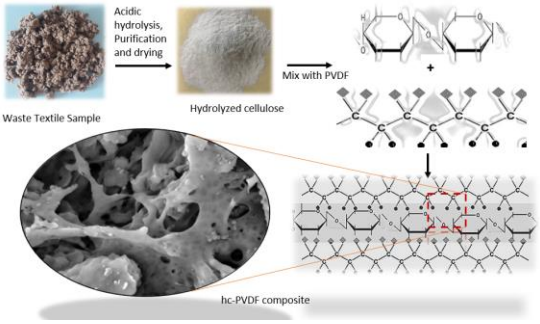

INTRODUCTION

Regeneration of waste materials became a vital issue worldwide in the context of keeping under control the carbon releasing rate into the atmosphere. Cellulose is an eco-friend material thanks to its large amount on earth, biodegradability-biocompatibility, and reusability. The well-known cellulosic sources consist of many kinds of wood and plant-based biomass with bacterial cellulose mainly. Although it seems unlimited, cellulose sources may also run out if they were not handled properly. The concern about the regeneration of used cellulosic sources increased. Nano cellulose (NC) was obtained from the viscose yarn waste by a simple acid hydrolyze method without pretreatment.[1] The particles which have 42 nm average pore size, and 87% crystallinity were obtained. Cellulose nanocrystals (CNC) were separated by 50, 60 and 64% concentrated acid hydrolyze at 60-75 min. of alkaline treated cotton waste.[2] Higher crystal structured nano cellulose with 177 nm long was obtained from the raw cotton source.[3] It was reported that the hydrophilicity of obtained cellulose samples increased whereas thermal stability of samples decreased. Soy hulls, cotton linter, cotton wool, and mercerized textile waste are the other cellulose sources for the obtaining of recycled nano cellulose crystals with acid

* Corresponding author: huseyin.gumus@bilecik.edu.tr

hydrolyze and 2,2,6,6-tetramethyl piperidinyloxy (TEMPO) oxidation methods.[4–8] The facile and one-step extraction method of nano-micro cellulose encouraged the applications of cellulose. Antibacterial Ag containing poly lactic acid (PLA) matrix was synthesized by cellulose support with a 1% mass ratio.[9] Cellulose nanocrystals obtained by acidic hydrolyzing of cellulose membrane were added to poly(vinylidene fluoride) (PVDF) filtration membrane to improve the antifouling effect.[10] Hydrophilic NC additive enhanced the permeability and antifouling properties of the membrane by optimizing the microstructure. An effective oil/water separator dual-layered and hydrophobic-hydrophilic coated PVDF copolymer with hexafluoropropylene membrane (PVDF-HFP-PVDF-HFP-CNC) was prepared by using CNC additives.[11–13] On the other hand with the addition of NCC (nano cellulose crystals), reinforced and electrochemically improved separation membranes were successfully synthesized for Li-ion batteries.[14] PVDF, phosphate, and cellulose acetate combination presented improved electrochemical performance with porous and flame retardant property.[15] Cellulose in micro or nano form is preferred as an effective additive on functional materials such as drug carriers, filtration, and phase separation membranes to set desired microstructure, pore size, and distribution, thermal and mechanical resistance with other specific properties.[16] Besides, sensors, packaging, medical equipment, health applications, cosmetics, flexible electronics, photovoltaics and 3D printings are some other applications in which cellulose was used as an additive in the composite or its raw form.[17,18] Crystal cellulose provides practical application opportunities thanks to its functional hydroxyl and carbonyl groups which interact with targeted ions or molecules in the aqueous area. All-Cellulose (product name in the mentioned study), cellulose-containing layered membranes, TEMPO-oxidized cellulose membranes were used for the Au(II), Co(II), Fe(III) and dye adsorption.[19] All-cellulose membrane provided the highest metal removal, high catalytic hydrogenation of rhodamine-B (RhB) however low methylene blue (MB) hydrogenation. For tellurium removal, zinc containing self-cross linked ZIF-L-SC cellulose membrane was used.[20] Cellulose-based temperature sensitivity molecular imprinted hydrogel composite was performed for specific recognition and enrichment of paclitaxel.[21] Uranium adsorption was achieved from simulated seawaters with amidoxime modified polyacrylonitrile (PAN) grafted cellulose fiber membranes successfully.[22] Cellulose-based composites are promising candidate for obtaining efficient dye and cation adsorption and filtration systems. There are lots of adsorption materials and applications for water treatment in the literature. However low cost, easy to obtain, and likely to be high performance adsorbents are the most preferred ones. In this study, we aimed to prepare low-cost adsorbent material from recycling of textile waste. We investigated the adsorption performance of textile waste-based hydrolyzed cellulose (hc)-PVDF composites (hc-P). The effect of hc and PVDF ratio on the composite structure were investigated. The optimal combination was determined by analyzing the crystal structure, functional groups, and surface properties with XRD, FT-IR, BET, and SEM investigations. Dye adsorption experiments were conducted in the batch systems under different temperatures and adsorbent amounts. The hc obtaining procedure, hc-P composite preparation, and their dye removal performances were investigated.

RESULTS AND DISCUSSION

Characterization of composites

The 50hc-P composite which consists of 50% hc and 50% PVDF was identified as the optimal composition having the most hc content and showing good physical and adsorption performance. The choosing criteria of the sample was determined in terms of the hc% ratio with high physical durability and SEM, FT-IR, BET characterization results. With 100% hc composite, it was aimed to prepare an adsorbent from completely recycled material, which does not require any other chemicals in the synthesis phase. But without a binder 100% hc composite could not be obtained. On the other hand, the 75hc-P composite could not be reused as an adsorbent due to its very low physical strength. Therefore, the reusability of only 50hc-P for dye adsorption was investigated.

The X-ray diffraction patterns of bare PVDF and hc-P composites are shown in Figure 1. Characteristic 2θ=18.58, 20.21, 27.2 peaks corresponding to the α-phase of PVDF were observed at all diffractograms. The clear peak of 50hc-P at 22.7 with the peaks at the range of 14-17 represent characteristic cellulose structure.[5] These sharp peaks point out well crystallinity of hydrolyzed cellulose because of the removal of the amorphous structure by acid treatment. Sufficient interaction

of PVDF and hc could be understood from presence of main PVDF peaks on the composite structure. The intensity of 27.2 peak decreased while new peak emerged at 34.5. That was attributed to cellulose crystal and new mixed crystal formations. Composites were analyzed by FT-IR to investigate molecular interaction of functional groups. Asymmetric and symmetric CH_2 vibrations of PVDF were observed at 3024 and 2982 cm^{-1} clearly (Figure 2). The bands at around 1401 and 1180 cm^{-1} were attributed to CH_2 rocking and C-C absorptions respectively. Characteristic CH and CF stretching vibrations absorptions of PVDF were observed at 874 and 840 cm^{-1}.

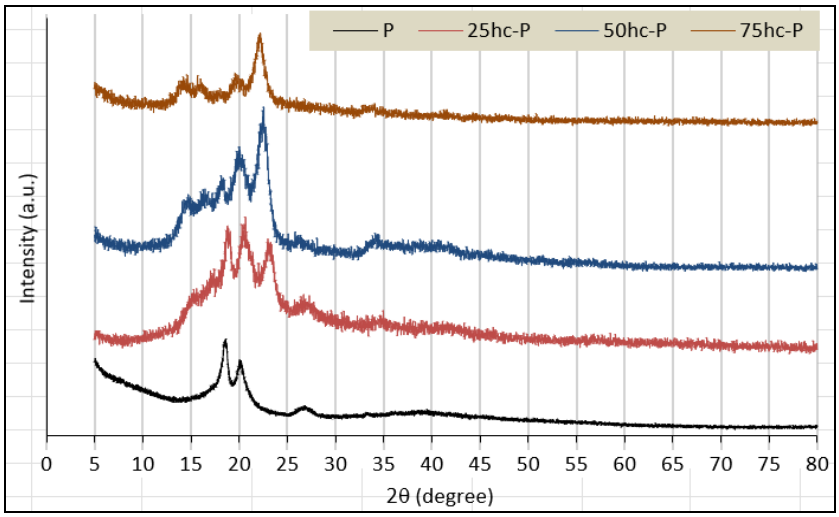

Fig. 1 – XRD patterns of P and hc-P composites.

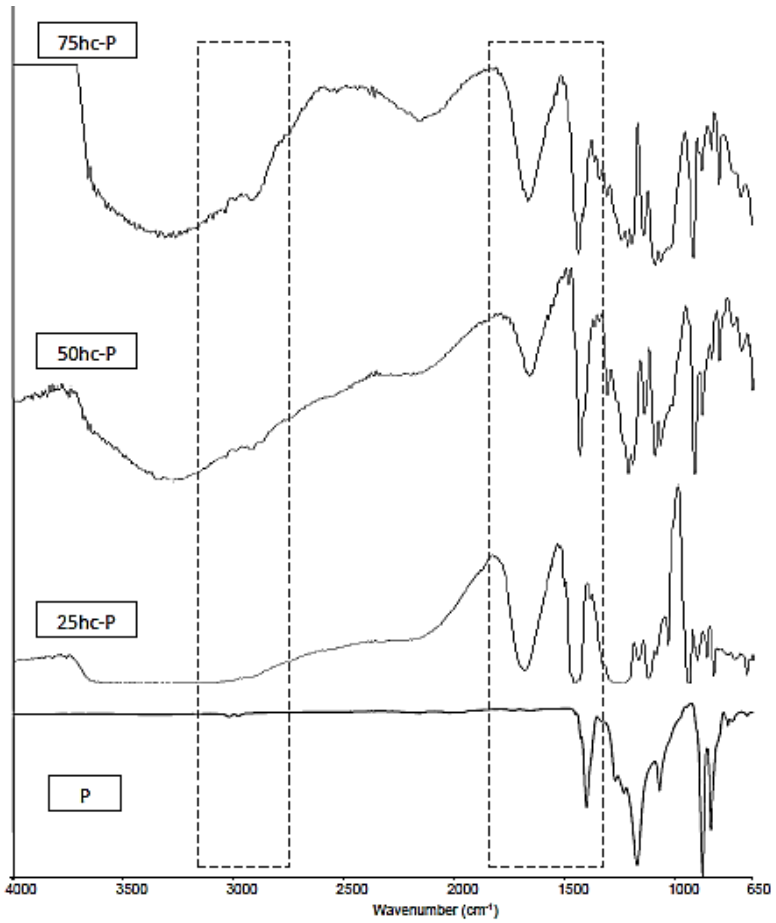

Fig. 2 – FT-IR spectrums of P and hc-P composites.

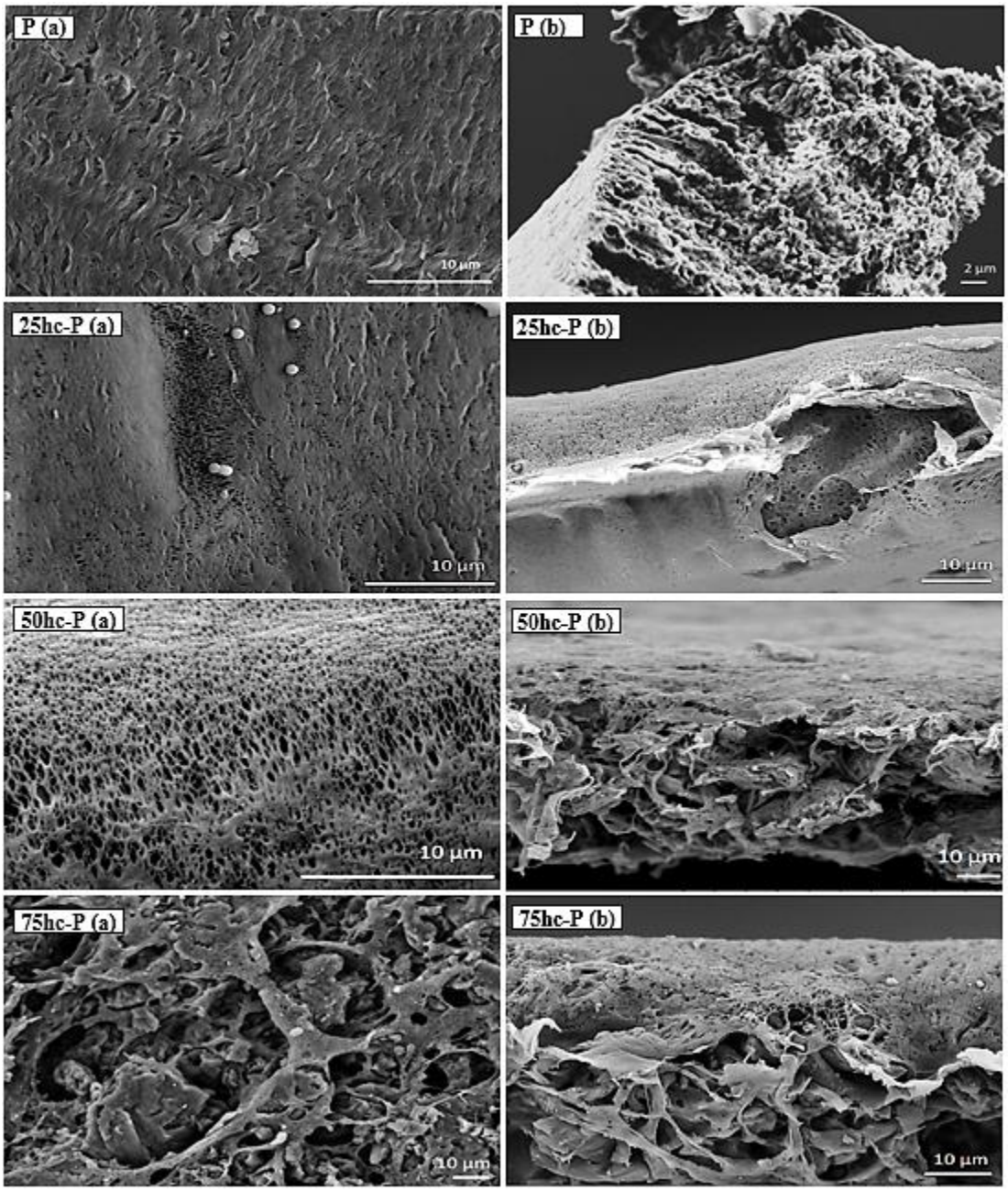

Fig. 3 – Surface (a) and crosssection (b) SEM images of P and hc-P composites.

These specific PVDF bands, 1402, 1180, 874, and 840 cm^{-1} were emerged at the hc-P spectrum with small shifts except 3024 and 2982 cm^{-1}. A broad peak corresponds O-H stretching was emerged at around 3400 cm^{-1}. The 1634 cm^{-1} band may be attributed to bending vibrations of H-O-H groups that represents the hydrophilic nature of cellulose.[1,23] At the spectrums, newly emerged absorption bands that pointed out the presence of hc with the bands showing the retaining of PVDF structure are clear evidence for hc and PVDF combination to form a composite material. It is understood from both XRD and IR analyses that the characteristic diffraction patterns and absorption bands of PVDF decrease or disappear after 50 percent hc addition.

To investigate the effect of hc addition to PVDF the SEM analysis of pure PVDF and flat sheet composites were obtained and presented in Figure 3. As could be seen from the surface and cross section images that pure PVDF has compact structure with small pores and sponge like seeds. While compression has not yet started on the surface of 25hc-P, in contrast, 50hc-P presented a great number of mixes of small-larger holes and porous structures even its sticky and pressed cross

section. The sieve-like structure of composite could be seen clearly after the hc addition, and the channels were not blocked due to agglomeration. However, structure shape changed with increasing hc ratio. The lattice on the 75hcP surface, which is dense and different from the PVDF texture, formed due to an increased amount of hc. Different characteristics of PVDF and hc against water during the phase inversion may be responsible for such an arrangement. While hc increased the wettability of the composite increased thanks to its hydrophilic feature and it tended to separate from the hydrophobic PVDF during phase separation.[24] However, this dissociation tendency does not prevent the formation of composite, but only resulted in agglomeration that causes the formation of large pores. Since the hc and PVDF mixed well with each other in the solution form, it is not possible to fully separate in the composite. On the contrary, addition of hc increased the hydrophilicity of PVDF composites. That is important and necessary for sufficient water pertaining composite formation.[25]

The surface properties of P and hc-P composites could be seen from the Table 1. BET analysis results was supported by wettability (WU%) and porosity (PO%) data. Hydrolyzed cellulose addition resulted in large number of pores in the composites consisted with the explanations of SEM results. An improvement on the surface area of 50hc-P (15.83 $m^2.g^{-1}$) was achieved compared with P (4.11 $m^2.g^{-1}$). A very small decrease in the surface area was noted with 75hc-P. That was due to the nature of formation of dense and viscose structure when the incorporation of an additive to polymeric matrix. Here also the incorporation resulted in more compressed and denser yield compared with raw polymer.

Smaller pores and pore volumes are the evidence of the presence of many small-medium size pores with increasing WU% and PO% values of samples. The increase on the water uptake capacity is proportional with water penetrating inside the pores. For this, there should be large pores that can hold a lot of water, or many small pores are required. The increasing water uptake (from 57.2 to 58.6%) is significant effect on the filtration, adsorption and catalytic effect composites or membranes. Higher water uptake capacity was obtained with increasing PO% from 65.5 to 69.2 and 70.1 for P, 50hc-P and 75hc-P respectively. In this way, it may be possible to expose more liquids with the active sites of composite. As far as 50hc-P, 75%hc-25% PVDF composition (75hc-P) also presented a useful composite material with moderate surface properties.

Dye adsorption performances of P and 50hc-P samples

Dye adsorption studies of P and hc-P samples were conducted with 100 $mg.L^{-1}$ MO model chemical . Effect of adsorbent dosage on the MO adsorption performance of hc-P composites were investigated. To understand effect of temperature on the adsorption performance, studies were conducted at 308, 318 and 328 K, in addition to the studies carried out at 298 K. However, any remarkable change was not observed by increasing temperatures so, 298 K was decided as adsorption temperature for this study. After the contacting of MO with 50 mg adsorbent in conical flask at 150 rpm stirring rate, approximately 5 ml solution was taken and analyzed by UV spectrometer.

The pH of the aqueous medium was studied at approximately 7.5, the pH value of the solution when it was first prepared, without any other adjustments. Initial dye concentration and adsorption time were applied as 100 $mg.L^{-1}$ and 1 hour respectively for MO adsorption.[26,27] Optimum conditions can be determined by studying the pH, initial dye concentration, and contact time parameters. However, the aim of this study was primarily to investigate the physical properties and dye removal performance of the hc containing adsorbent. Determining the optimum conditions of adsorption is the subject of another study. Since flat sheet adsorbent consisting of 100% hc is not prepared without the use of binding chemicals, and 75hc-P has poor physical strength, only 50 hc-P composite was investigated for the reusability performance.

Table 1

BET area, water uptake (WU%) and porosity percentages of P and hc-P composites

Sample	S_{BET} ($m^2.g^{-1}$)	V_{total} ($cm^3.g^{-1}$)	Pore width (nm)	WU%	PO%
P	4.11	0.042	6.3	57.2	65.5
25hc-P	4.68	0.026	6.6	57.5	66.0
50hc-P	15.83	0.025	5.8	58.6	69.2
75hc-P	15.06	0.017	3.9	58.0	70.1

S_{BET} :BET surface area
V_{total}: Total pore volume.

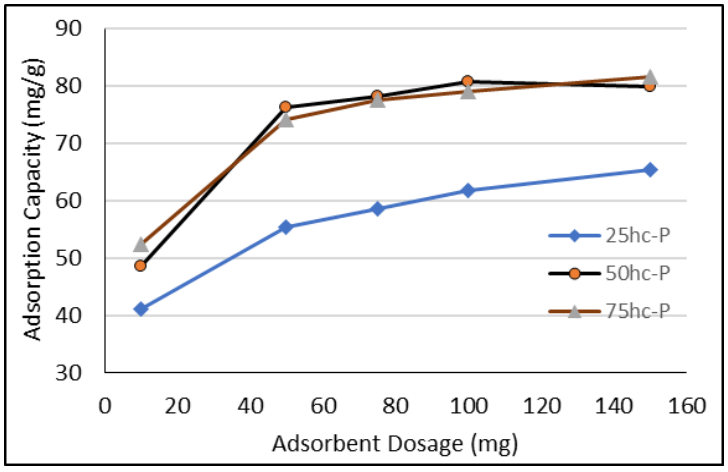

Fig. 4 – MO adsorption performance of hc-P composites (it was 24.22 $mg.g^{-1}$ for 50 mg P).

The effect of adsorbent dosage on the adsorption performances of hc-P was investigated and results were presented in Fig. 4. MO adsorption sharply increased from 48.48 $mg.g^{-1}$ to 76.37 $mg.g^{-1}$ with increased adsorbent amount from 10 to 50 mg for all composites and it was reached the highest value of 81.6 for 75hcP. But the linear increase in the amount of adsorbed MO versus the amount of adsorbent changed to a decreasing trend after 75 mg. That was due to the saturation of active sites on the adsorbent after the first interaction. The surface properties of adsorbent, molecular interaction, and charges in the aqueous area have high impact on the adsorption mechanism. From the characterization results, it was understood that the pore structure of 50hc-P and 75hc-P shrinked, but its pore number increased. Small pores may have prevented the entry of the second dye molecules after the first molecule penetration. Thus, the rate of increase in the amount of adsorbed substance was less than the amount of adsorbent. Despite the increasing amount of adsorbent, the performance of 25hc-P was almost half of the other composites. This is a clear proof that hc improves the adsorption performance of PVDF.

Different charged molecules and lower initial dye concentration may be effective on to increase adsorption with increasing adsorbent amount. It was concluded that 50-75 mg adsorbent was the ideal adsorbent value under the specified conditions for hc-P composites. The formation of 50hc-P composite consisting of 1:1 hc and PVDF was investigated, and a durable structure was obtained. From the characterization results, the presence of interacting functional groups in the composite were seen. It has been understood that it is effective in removing the dyestuff from the aqueous solution under the studied conditions, and it is promising for higher rate of dyestuff, organic pollution, or heavy metal adsorption under optimum conditions. This study is a good example of the disposal of industrial wastes by converting them into useful products. 75hc-P can also be used as an adsorbent in a batch system, but it is unlikely to be used in a pressure filtration system due to its low physical strength.

Regeneration

Reusability of composites were investigated after washing with 0.5 $mg.L^{-1}$ HCl solution. After 5 cycles there was no prominent change in the adsorption capacity of samples Fig. 5. A small amount of increase and decrease observed for the MO adsorption performances of composites may be the result of the deep penetration of a very small number of dye molecules inside the pores. As far as the remarkable adsorption value the durability of the adsorbent is a vital issue for feasible and sustainable adsorption. Despite the nature of hydrolyzed cellulose being easily affected by the acidic environment, the composite structure formed by hc with PVDF has high acid resistance. Thus, 50hc-P could be seen as a suitable adsorbent material for pollution removal from an aqueous environment for both batch and membrane filtration systems.

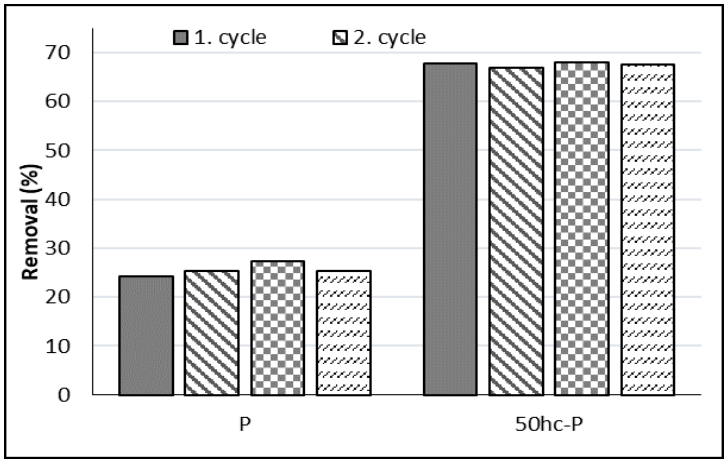

Fig. 5 – Reusing performances of P and 50hc-P composite.

MATERIALS AND METHODS

Materials

Textile waste materials for cellulose sources were obtained from UŞAK organized Industrial Zone, Turkey. H_2SO_4, poly(vinylidene fluoride) (PVDF, Mw ~107,000 $g.mol^{-1}$) and N, N-Dimethylacetamide (DMAc) were purchased from Sigma Aldrich and used without any processing. Methyl orange (MO) (from Sigma Aldrich) aqueous solution was used as a model pollutant and used directly.

Preparation of hydrolyzed cellulose-PVDF composites

Textile waste remnants were firstly washed with ethanol and 80-90°C hot water to remove dirt and dye. It was dried at 60°C for 24 h. 10 g sample was put into a glass and sulfuric acid (H_2SO_4, 64% w/w) was added by stirring magnetically. Until to obtain a white slurry with small particles, acid was added and after that, it was stirred for 1 hour at 40-50°C. Cold water was added to complete hydrolysis, and the slurry was waited to precipitate. It was washed and decantated five times until the obtain neutral pH values. The white powder was dried at 60°C and stored to use as a composite component.

3 g of dry hydrolyzed cellulose and PVDF were weighted and dissolved in DMAc separately by ultrasonication to obtain a 14% mass ratio in terms of hc and PVDF to solvent. Hc and PVDF solutions were mixed at the ratio of 3:1, 1:1, 1:3 respectively and it was stirred at 250 rpm at 65°C for 12 hours. The mixture was waited for 10 minutes to prevent air bubbles and cast onto flat surface (15 cm x 15 cm) uniformly with a 300 μm casting knife at 25°C. After exposure to air for 10 seconds, the glass plate was quickly immersed in a coagulation bath. The schematic representation of reparation steps and details were similar to our former study.[24] Membranes were dried for characterization while adsorption membranes were stored in distilled water for dye adsorption. Composites containing hc at the rate of 0, 25, 50, 75% according to the total mass of combination were determined as P, 25hc-P, 50hc-P, and 75hc-P respectively.

Characterization of Composites

Structural changes at crystallinity and functional groups of prepared samples were analyzed by XRD (Rigaku 2000) at 2θ=2-80° with $2°.min^{-1}$ scanning speed and Perkin Elmer FT-IR over a range of 4000-400 cm^{-1}. Morphology of composites was imaged by scanning electron microscopy (SEM) at 10 kV (Carl Zeiss ULTRA Plus). The surface area of composites was determined by TriStar II 3020 Version 3.02 BET device. The initial and final concentrations of dye solutions were determined by a UV-visible spectrometer (Shimadzu, 2550) at 660 nm wavelength for MO.

Dye Adsorption Experiments

Adsorption performances of composites were tested in a conical flask by the batch technique. 50 mL MO aqueous solutions (50-150 ppm initial concentrations) and 0.01-0.1 g adsorbent were put into an adsorption cup, and it was stirred at 150

rpm for 1-3 h. Adsorption temperature and pH value of solutions were adjusted at 298-328 K and pH 7.5 as solution pH. After the equilibrium, samples were filtered, and the amount of MO in the filtrate was analyzed by a UV-vis spectrometer at 660 nm. Adsorption capacity Q_e ($mg.g^{-1}$) and adsorption efficiency EAD (%) of adsorbents were calculated by equations 1 and 2.[28,29]

$$Q_e = \left(\frac{C_0 - C_e}{M}\right) xV \quad (1)$$

$$E_{AD}(\%) = \left(\frac{C_0 - C_{eq}}{C_0}\right) x100 \quad (2)$$

C_0 and C_e stand for initial and equilibrium dye concentration in $mg.L^{-1}$ respectively. M (g) and V (L) represent the amount of adsorbent and the volume of dye solution, respectively. The reusability of adsorbents was investigated after washing and rinsing the filtrated adsorbents with an acid solution (0.5 $mol.L^{-1}$ HCl, 25 mL). The adsorbents were used 5 times. Adsorption capacities of all samples were calculated and evaluated according to equations 1 and 2.

CONCLUSIONS

In this study, separation of cellulose from textile waste products and composite formation with PVDF were conducted. Prepared samples were analyzed by FT-IR, XRD, SEM, and BET analyses. From the peaks observed in the XRD diffraction pattern and from the SEM images, it was concluded that the best structural composition in terms of adsorption performance, durability, and hc amount was 50hc-P. The MO adsorption performance of P and 50hc-P in the batch system was recorded as 24.47 and 76.37 $mg.g^{-1}$, respectively. The satisfactory MO adsorption performances of 50hc-P composite proved that it will be an effective adsorbent material to remove impurities from water with its advantages of reusability, low cost, and easy application. The presence of homogeneous morphological and crystalline structure and functional groups determined by structural analysis is promising that the composite can be used as a membrane in filtration and fuel cells.

REFERENCES

1. K. S. Prado, D. Gonzales and M. A. S. Spinacé, *Int. J. Biol. Macromol.*, **2019**, *136*, 729–737. https://doi.org/10.1016/j.ijbiomac.2019.06.124.
2. M. M. Á. D. Maciel, K. C. C. de C. Benini, H. J. C. Voorwald and M. O. H. Cioffi, *Int. J. Biol. Macromol.*, **2019**, *126*, 496–506. https://doi.org/10.1016/j.ijbiomac.2018.12.202.
3. J. Mehdi, O. Reza, D. Yalda, O. Kristiina, D. Alain, H. Yahya and D. Reza, *Cellulose*, **2015**, 22, 935–969. doi 10.1007/s10570-015-0551-0.
4. W. P. Flauzino Neto, H. A. Silvério, N. O. Dantas and D. Pasquini, *Ind. Crops Prod.*, **2013**, *42*, 480–488. https://doi.org/10.1016/j.indcrop.2012.06.041.
5. A. A. Oun and J. W. Rhim, *Carbohydr. Polym.*, **2015**, *127*, 101–109. https://doi.org/10.1016/j.carbpol.2015.03.073.
6. G. Morandi, L. Heath and W. Thielemans, *Langmuir*, **2009**, *25*, 8280–8286. https://doi.org/10.1021/la900452a.
7. E. Abraham, B. Deepa, L. A. Pothan, M. Jacob, S.Thomas,U. Cvelbar and R. Anandjiwala, *Carbohydr. Polym.*, **2011,** *86*, 1468-1475. https://doi.org/10.1016/j.carbpol.2011.06.034.
8. M. Cheng, Z. Qin, Y. Chen, J. Liu Z. Ren, *Cellulose*, **2017**, *24*, 3243–3254. https://doi.org/10.1007/s10570-017-1339-1.
9. E. E. Yalcinkaya, D. Puglia, E. Fortunati, F. Bertoglio, G. Bruni, L. Visai J. M. Kenny, *Carbohydrate Polymers*, **2017**, 1557–1567. https://doi.org/10.1016/j.carbpol.2016.11.038.
10. J. Lv, G. Zhang, H. Zhang, C. Zhao and F. Yang, *Appl. Surf. Sci.*, **2018**, *440*, 1091–1100. https://doi.org/10.1016/j.apsusc.2018.01.256.
11. O. Makanjuola, F. Ahmed, I. Janajreh and R. Hashaikeh, *J. Memb. Sci.*, **2019**, *570–571*, 418–426. https://doi.org/10.1016/j.memsci.2018.10.028.
12. F. Ejaz, B. Singh, N. Hilal and R. Hashaikeh, *Desalination*, **2014**, *344*, 48–54.
13. X. Wang, W. Cheng, D. Wang, X. Ni and G. Han, *J. Memb. Sci.*, **2019**, *575*, 71–79. https://doi.org/10.1016/j.memsci.2018.12.057.
14. M.Bolloli, C. Antonelli, Y. Molméret, F. Alloin, C. Iojoiu, J. Y. Sanchez, *Electrochim. Acta*, **2016**, *214*, 38–48. https://doi.org/10.1016/j.electacta.2016.08.020.
15. Y. Chen, L. Qiu, X. Ma, L. Dong, Z. Jin, G. Xia, P. Du and J. Xiong, *Carbohydr. Polym.*, **2020**, *234*, 115907. https://doi.org/10.1016/j.carbpol.2020.115907.
16. I. Abdelmalek, M. Mouffok, L. Bennabı, A. Meslı, K. Guemra and El H. Belarbı, *Rev. Roum.Chim.*, **2021**, *66*, 527–536. Https://Doi.Org/10.33224/Rrch.2021.66.6.05.
17. B.-I. Dogaru, M.-C. Popescu and B. C. Simionescu, *Rev. Roum. Chim.*, **2017**, *62*, 599–604.
18. L. Jasmani and W. F. Thielemans, *J. For. Res.*, **2018**, *7*, 1–8. https://doi.org/10.4172/2168-9776.1000222.
19. D. Georgouvelas, H. N. Abdelhamid, J. Li and U. Edlund, *Carbohydr. Polym.*, **2021**, *264*, 118044. https://doi.org/10.1016/j.carbpol.2021.118044.
20. Z. Li, M. Gou, X. Yue, Q. Tian, D. Yang, F. Qiu and T. Zhang, *J. Hazard. Mater.*, **2021**, *416*, 125888. https://doi.org/10.1016/j.jhazmat.2021.125888.
21. J. Cao, X. Wu, L. Wang, G. Shao, B. Qin, Z. Wang, T. Wang and Y. Fu, *Int. J. Biol. Macromol.*, **2021**, *181*, 1231–1242. https://doi.org/10.1016/j.ijbiomac.2021.05.095.
22. Y. Wang, Y. Zhang, Q. Li, Y. Li, L. Cao, W. Li, *Carbohydr. Polym.*, **2020**, *245*, 116627. https://doi.org/10.1016/j.carbpol.2020.116627.
23. D. T. T. Nu, N. P. Hung, C. Van Hoang and B. Van der Bruggen, *Appl. Sci.*, **2019**, *9*, 3347-3362 https://doi.org/10.3390/app9163347.

24. H. Gumus, *J. Turkish Chem. Soc. Sect. A Chem.*, **2020**, *7*, 361–374. https://doi.org/10.18596/jotcsa.610886.
25. B. Ma, J. Yang, Q. Sun, W. Jakpa, X. Hou, Y. Yang, *J. Mater. Sci.*, **2017**, *52*, 9946–9957. https://doi.org/10.1007/s10853-017-1150-2.
26. S. K. Dutta, M. K. Amin, J. Ahmed, M. Elias and M. Mahiuddin, *South African J. Chem. Eng.*, **2022**, *40*, 195–208. https://doi.org/10.1016/j.sajce.2022.03.006.
27. A. Yadav, R. V. Patel, C. P. Singh, P. K. Labhasetwar and V. K. Shahi, *Colloids Surfaces A Physicochem. Eng. Asp.*, **2022**, *635*, 128070. https://doi.org/10.1016/j.colsurfa.2021.128070.
28. P. A. R. De Sousa, L. T. Furtado, J. L. L. Neto, F. M. De Oliveira, J. G. M.; Siqueira, L. F. Silva and L. M. Coelho, *Brazilian J. Anal. Chem.*, **2019**, *6*, 14–28. https://doi.org/10.30744/brjac.2179-3425.AR.119-2018.
29. Z. Li, H. Hanafy, L. Zhang, L. Sellaoui, M. Schadeck Netto, M. L. S. Oliveira, M. K. Seliem, G. Luiz Dotto, A. Bonilla-Petriciolet and Q. Li, *Chem. Eng. J.*, **2020**, *388*, 124263 https://doi.org/10.1016/j.cej.2020.124263.